

*Supporting information (SI) for*

**SnO<sub>2</sub>/CoS<sub>1.097</sub> heterojunction as a green electrocatalyst for  
hydrogen evolution linking to assistant glycerol oxidation**

Xinjie Xie<sup>a</sup>, Chunyong Zhang<sup>a</sup>, Meng Xiang<sup>a</sup>, Chengbin Yu<sup>b</sup>, Wangxi Fan<sup>a,\*</sup>, Shuang Dong<sup>c,\*</sup>, and Zhou Yang<sup>a,\*</sup>

<sup>a</sup>. Department of Chemistry and Chemical Engineering, Jiangsu University of Technology, Changzhou 213001, China.

<sup>b</sup>. Research Institute of Advanced Materials (RIAM), Department of Materials Science and Engineering, Seoul National University, Seoul 08826, Republic of Korea.

<sup>c</sup>. School of Chemical Engineering and Materials, Changzhou Institute of Technology, Changzhou 213032, China.

\*Correspondences: Wangxi Fan, [fwx@jsut.edu.cn](mailto:fwx@jsut.edu.cn); Shuang Dong, [dongs@czu.cn](mailto:dongs@czu.cn); Zhou Yang, [zhouyang@jsut.edu.cn](mailto:zhouyang@jsut.edu.cn).

## Characterizations

The microstructure was observed by a Field-emission scanning electron microscope (FE-SEM, Sigma 500) with an energy dispersive spectrometer (EDS) and Transmission electron microscopy (TEM, JEM-2100) with selected area electron diffraction (SAED). The chemical properties were scanned by X-Ray Diffraction (XRD, X'PERT POWDER, scanning rate is  $10^\circ \text{ min}^{-1}$ ) and X-ray photoelectron spectroscopy (XPS, ThermoFisher Scientific ESCALAB 250, Al target). The  $\text{H}_2$  reduction curve was tested by  $\text{H}_2$ -TPR (Xianquan TP-5080, heating rate and cooling rate are both  $10^\circ\text{C min}^{-1}$ ). The contents of Co and S were measured by Inductive Coupled Plasma Emission Spectrometer Optical Emission Spectrometry (ICP-OES, Plasma 2000). The GOR product is characterized by  $^1\text{H}$  NMR (Bruker Avance III HD, 400 MHz, solution is  $\text{D}_2\text{O}$ ) and LC-MS (ThermoFisher U3000 liquid phase-QE mass spectrometry, flowing phase is water: methanol = 95:5).

The electrochemical measurements were performed by an electrochemical workstation (Chenhua, CHI 760E), tested programs include cyclic voltammetry (CV), linear sweep voltammetry (LSV), Chronopotentiometry (CP), electrochemical impedance spectroscopy (EIS), impedance–potential, and i-t curve.

For the three-electrode system, 2 mg of powder sample was dispersed in 200  $\mu\text{L}$  of mixed solution (deionized water: ethanol: Nafion = 2:7:1) to form ink, and then 10  $\mu\text{L}$  of this ink was dripped on a glass carbon electrode (GCE) and dried at room temperature, which was used as the working electrode, and Hg/HgO and graphite electrodes were used as the reference and counter electrodes, respectively. For the two-electrode system, the sample was mixed with acetylene black and polyvinylidene fluoride (PVDF) with a weight ratio of 8:1:1, and dispersed in N-methylpyrrolidone (NMP) to form slurry. The above slurry was coated on the nickel foam ( $1\times 1 \text{ cm}$ ) and dried. The electrolyte is 1 M KOH or 1 M KOH with organics.

The electrochemically active surface (ECSA) was calculated on the basis of the double-layer capacitance ( $C_{\text{dl}}$ ) theory,<sup>S1</sup>

$$\text{ECSA} = C_{\text{dl}} / C_s$$

Where the slope in the plot of current densities to scan rates stands for  $2C_{\text{dl}}$ , and  $C_s$

is 0.04 mF cm<sup>-2</sup>.

The Mott-Schottky (M-S) plot was performed according to the equation:  $\frac{1}{C^2} = \frac{2}{N_d e \epsilon \epsilon_0} \left( V - V_{FB} - \frac{KT}{e} \right)$

where C is the capacitance at the interface between semiconductor and electrolyte (F cm<sup>-2</sup>); e is the elementary charge (1.6×10<sup>-19</sup> C); ε is the relative dielectric constant (F m<sup>-1</sup>); ε<sub>0</sub> is the permittivity of the vacuum; N<sub>d</sub> is the carrier density (cm<sup>-3</sup>); V is the applied potential (V); V<sub>FB</sub> is flat band potential; K is Boltzmann's constant (1.38× 10<sup>-23</sup> F m<sup>-1</sup>); T is the absolute temperature (K).<sup>S2</sup>

In the above equation, the line plot of 1/C<sup>2</sup> to V is named M-S plot. The flat band potential (E<sub>fb</sub>) is the intercept by extrapolating the linear part of M-S plot to 1/C<sup>2</sup> = 0.

### Faradaic efficiency (FE) of GOR

The half-reaction formula for each product from GOR is listed as follows:

Product	Anode reaction formula	e <sup>-</sup> (mol)
Glycerol acid	CH <sub>2</sub> OH-CHOH-CH <sub>2</sub> OH + 5OH <sup>-</sup> → CH <sub>2</sub> OH-CHOH-COO <sup>-</sup> + 4H <sub>2</sub> O + 4e <sup>-</sup>	4
Glyceraldehyde	CH <sub>2</sub> OH-CHOH-CH <sub>2</sub> OH + 2OH <sup>-</sup> → CH <sub>2</sub> OH-CHOH-CHO + 2H <sub>2</sub> O + 2e <sup>-</sup>	2
Formic acid	CH <sub>2</sub> OH-CHOH-CH <sub>2</sub> OH + 11OH <sup>-</sup> → 3CHOO <sup>-</sup> + 8H <sub>2</sub> O + 8e <sup>-</sup>	8/3

FE of GOR is calculated based on the following equation:

$$FE (\%) = \frac{4 \times C_{glya} + 2 \times C_{glycd} + \frac{8}{3} \times C_{formic}}{Q} \times V \times F \times 100\%$$

Where, C<sub>glya</sub>, C<sub>glycd</sub>, and C<sub>formic</sub> are the concentration (mol L<sup>-1</sup>) of glycerol acid, glyceraldehyde, and formic acid; V is the volume of tested electrolyte (10 × 10<sup>-3</sup> L); F is the Faradaic constant (96485 C mol<sup>-1</sup>); Q is the total charge (C) passed during electrochemical reaction.<sup>S3</sup>

### DFT calculations

All the spin-polarized DFT calculations are performed by the Vienna Ab initio Simulation Package (VASP)<sup>S4</sup> with the projector augmented wave (PAW) method.<sup>S5</sup>

The exchange-function is treated using the generalized gradient approximation (GGA) with Perdew-Burke-Ernzerhof (PBE)<sup>S6</sup> function. The energy cutoff for the plane wave basis expansion was set to 500 eV. Partial occupancies of the Kohn–Sham orbitals were allowed using the Gaussian smearing method and a width of 0.05 eV and the spin polarization was considered. For k-space sampling,  $k_1 \times k_2 \times k_3$   $\Gamma$ -centered Monkhorst-Pack meshes were used, where  $k_n$  ( $n = 1,2,3$ ) was prepared as the mesh spacing near ( $2\pi \times 0.04 \text{ \AA}^{-1}$ ) to each direction. The self-consistent calculations apply a convergence energy threshold of  $10^{-4}$  eV, and the force convergency was set to 0.05 eV/ $\text{\AA}$ .

**Table S1.** The contents of Co and S tested by ICP-OES

Element	Co	S
Content (mg L <sup>-1</sup> )	7.14	4.26

**Table S2.** The contents of component

Component	C <sub>3</sub> H <sub>6</sub> O <sub>3</sub>	C <sub>3</sub> H <sub>6</sub> O <sub>4</sub>	HCOOH
Content (mol L <sup>-1</sup> )	0.037	0.027	0.029

**Table S3.** Comparison with other electrocatalysts in electrolyte with organic additions by two-electrode method.

Electrocatalyst	Electrolyte	Cell voltage (V) at 10 mA cm <sup>-2</sup>
Mn-CoSe <sub>2</sub> /CFC) <sup>S7</sup>	1 M KOH + 0.1 M glycerol	1.45
Ni <sub>3</sub> N-Ni <sub>0.2</sub> Mo <sub>0.8</sub> N <sup>S8</sup>	1 M KOH + 0.1 M glycerol	1.40
PtSA-NiCo LDHs/ NF <sup>S9</sup>	1 M KOH + 0.1 M glycerol	1.21
CNs@CoPt <sup>S10</sup>	1 M KOH + 10 mM glycerol	1.50
W-NiS <sub>2</sub> /MoO <sub>2</sub> @CC <sup>S11</sup>	1 M KOH + 0.33 M urea	1.372
Core-corona Co/CoP <sup>S12</sup>	1 M KOH + 0.5 M glucose	1.42
Ni-MoS <sub>2</sub> <sup>S13</sup>	1 M KOH + 0.3 M glucose	1.67
0.5 SnO <sub>2</sub> /0.5 CoS <sub>1.097</sub> (This work)	1 M KOH + 0.1 M glycerol	1.18

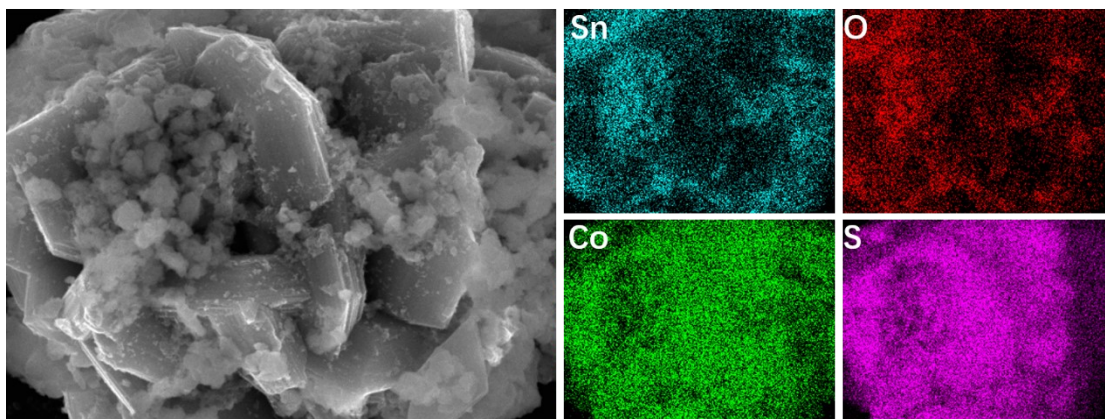


**Figure S1** The elemental mapping of 0.7 SnO<sub>2</sub>/0.3 CoS<sub>1.097</sub>.

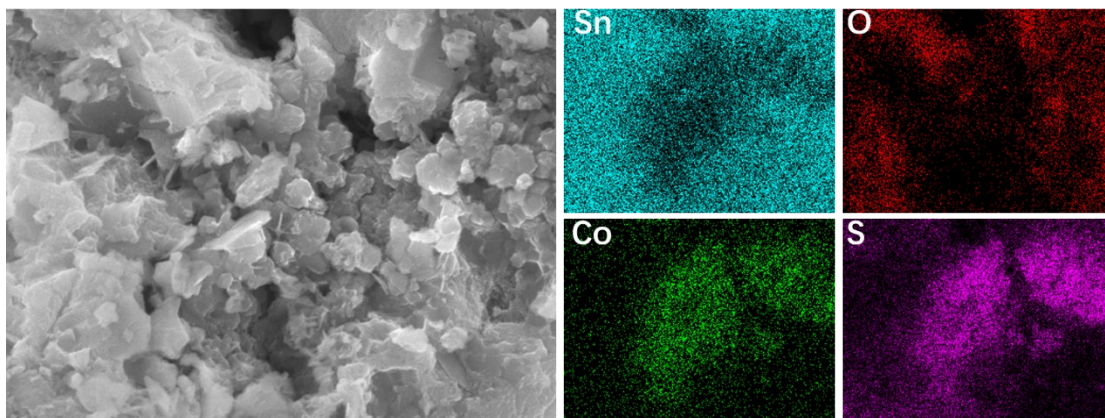


**Figure S2** The elemental mapping of 0.3 SnO<sub>2</sub>/0.7 CoS<sub>1.097</sub>.

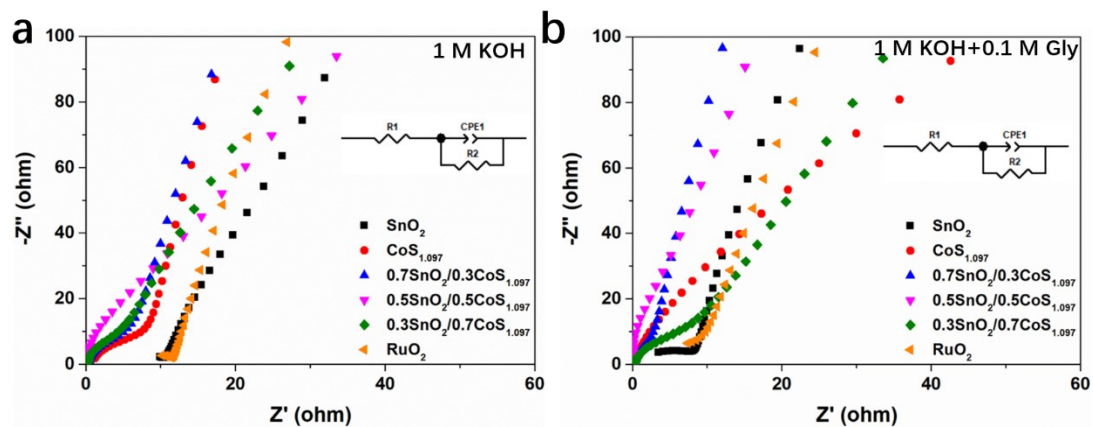


**Figure S3** The EIS plots of  $\text{SnO}_2$ ,  $\text{CoS}_{1.097}$ ,  $0.7 \text{SnO}_2/0.3 \text{CoS}_{1.097}$ ,  $0.5 \text{SnO}_2/0.5 \text{CoS}_{1.097}$ ,  $0.3 \text{SnO}_2/0.7 \text{CoS}_{1.097}$ , and  $\text{RuO}_2$  in 1 M KOH (a) and 1 M KOH + 0.1 M glycerol (b). (All the EIS test at Amplitude = 0.005 V from 1 HZ to  $10^5$  HZ.)



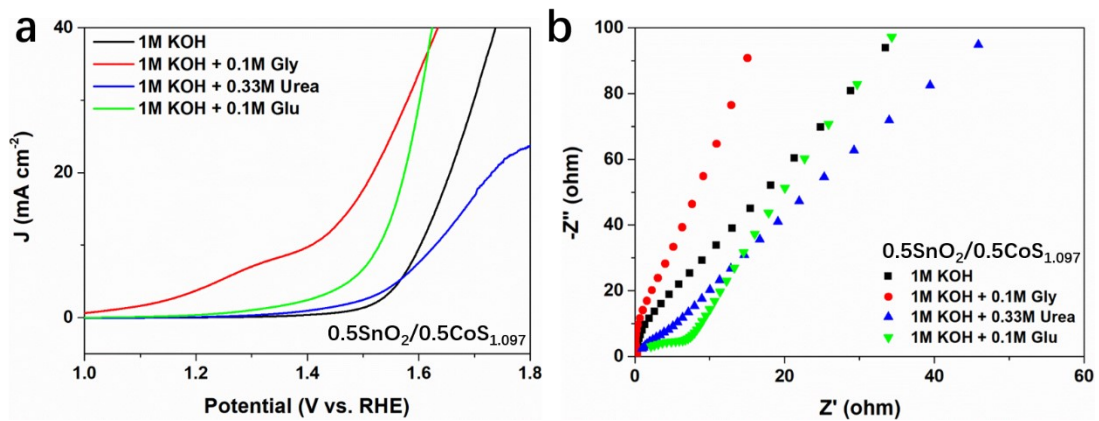


**Figure S4** The OER LSV curves (a) and EIS plots (b) of  $0.5\text{SnO}_2/0.5\text{CoS}_{1.097}$  in the different electrolytes.

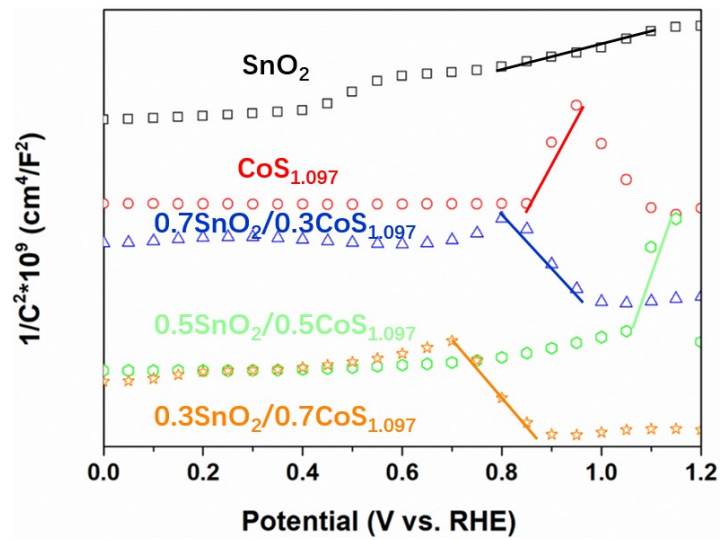


**Figure S5** The M-S plots of SnO<sub>2</sub>, CoS<sub>1.097</sub>, 0.7 SnO<sub>2</sub>/0.3 CoS<sub>1.097</sub>, 0.5 SnO<sub>2</sub>/0.5 CoS<sub>1.097</sub>, 0.3 SnO<sub>2</sub>/0.7 CoS<sub>1.097</sub> in 1 M KOH.

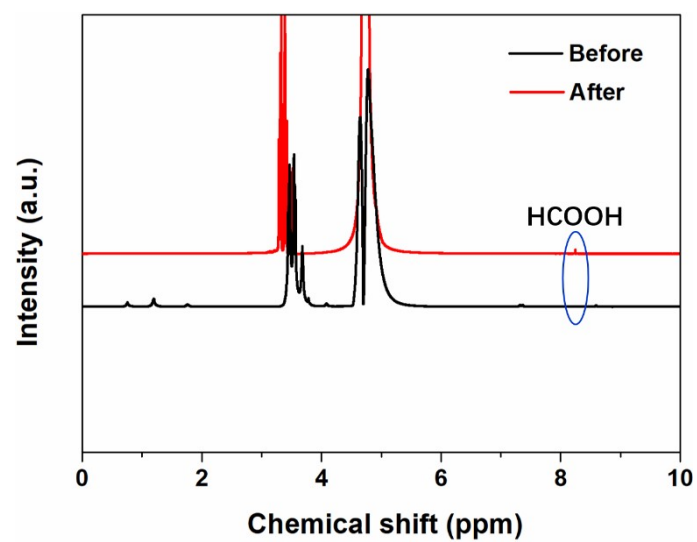


**Figure S6** The <sup>1</sup>H NMR of electrolyte of 0.5 SnO<sub>2</sub>/0.5 CoS<sub>1.097</sub> before and after GOR.

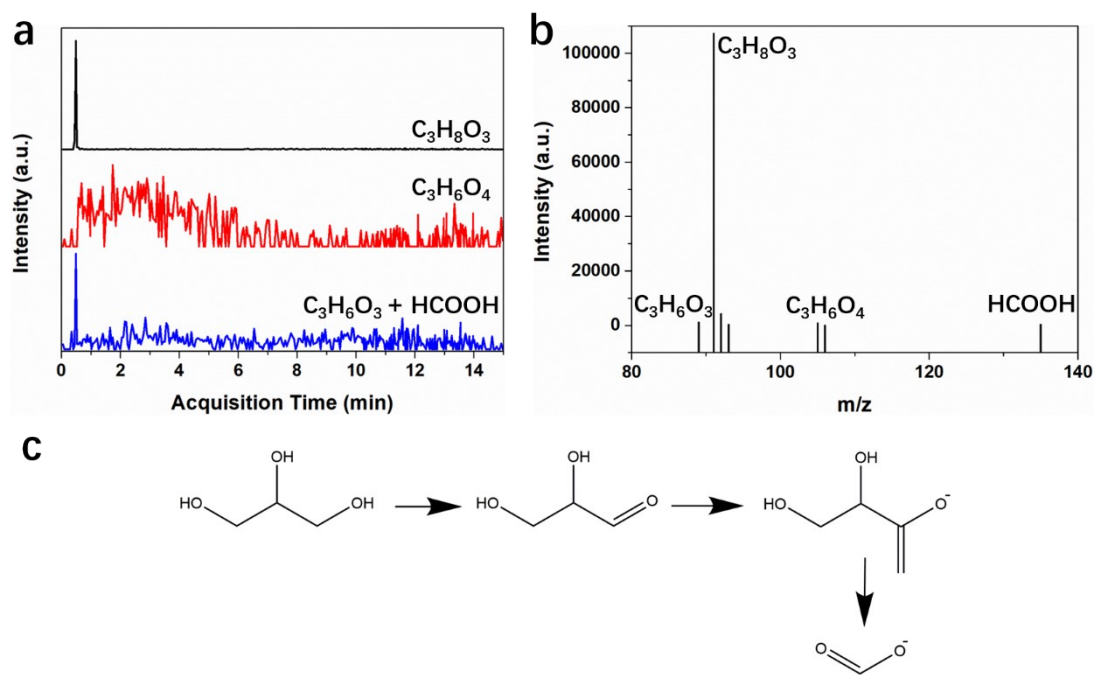


**Figure S7** (a, b) LS-MS of product after GOR of 0.5 SnO<sub>2</sub>/0.5 CoS<sub>1.097</sub>. (c) GOR formula of 0.5 SnO<sub>2</sub>/0.5 CoS<sub>1.097</sub>.

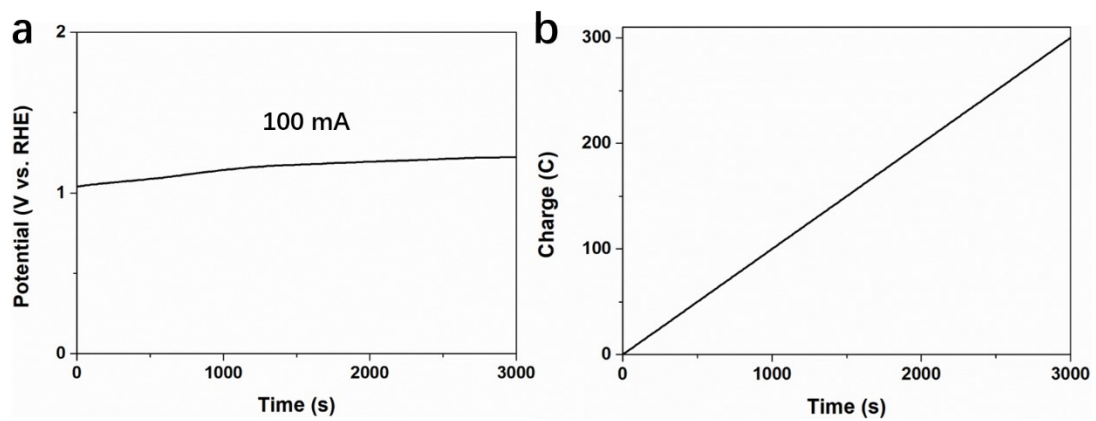


**Figure S8** (a) Chronopotentiometry curve of the 0.5 SnO<sub>2</sub>/0.5 CoS<sub>1.097</sub> at a constant current of 100 mA. (b) The plot of corresponding charge to time.

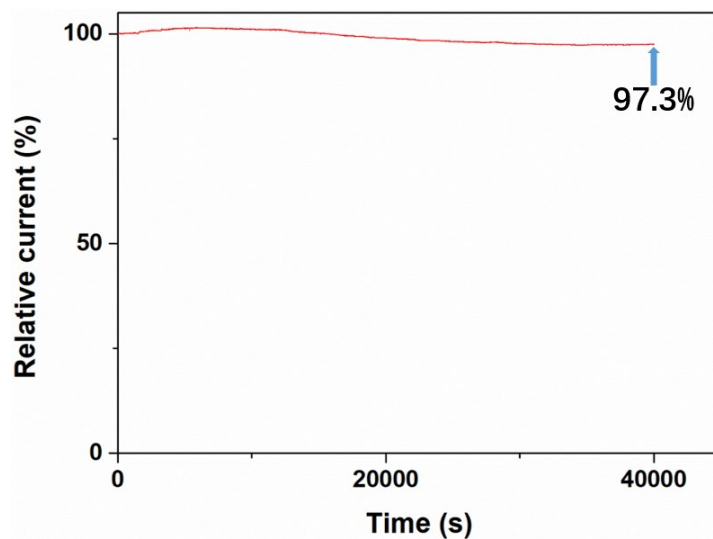


**Figure S9** I-t plot of 0.5 SnO<sub>2</sub>/0.5 CoS<sub>1.097</sub> in 1 M KOH + 0.1 M glycerol.

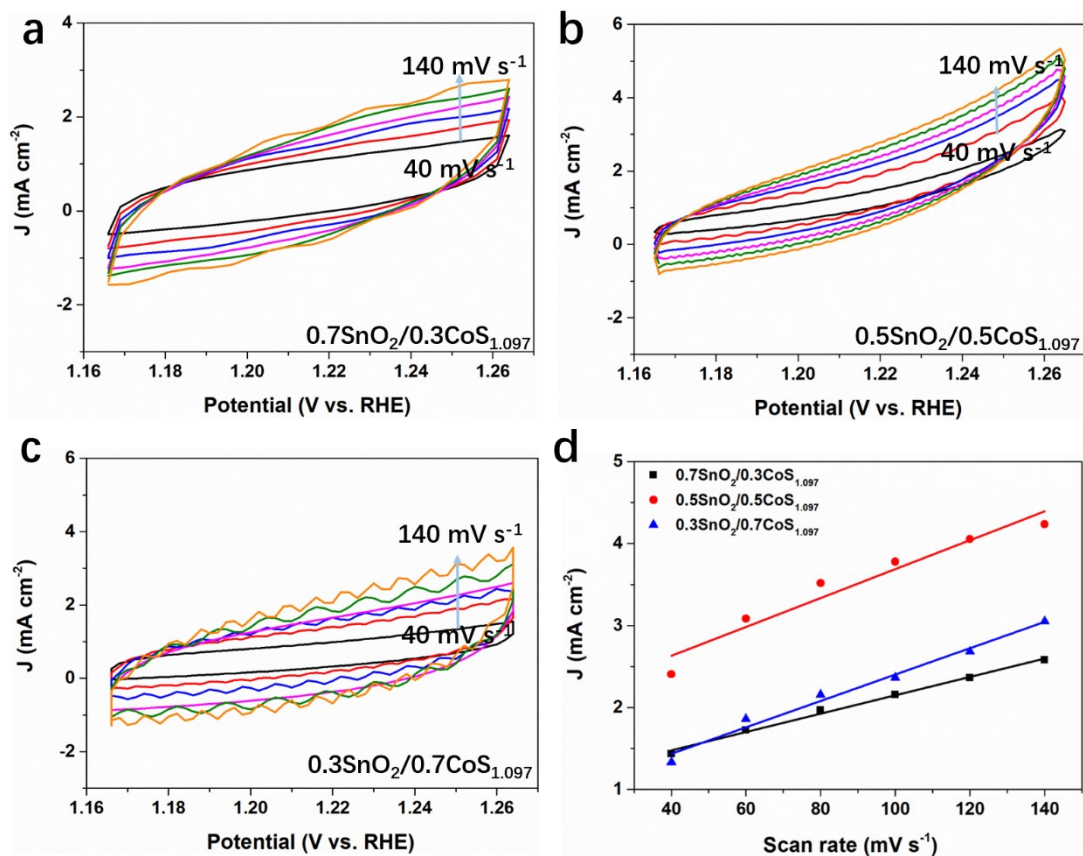


**Figure S10** The CV curves at different scan rates of (a) 0.7 SnO<sub>2</sub>/0.3 CoS<sub>1.097</sub>, (b) 0.5 SnO<sub>2</sub>/0.5 CoS<sub>1.097</sub>, and (c) 0.3 SnO<sub>2</sub>/0.7 CoS<sub>1.097</sub>. (d) The plots of current density to scan rates.

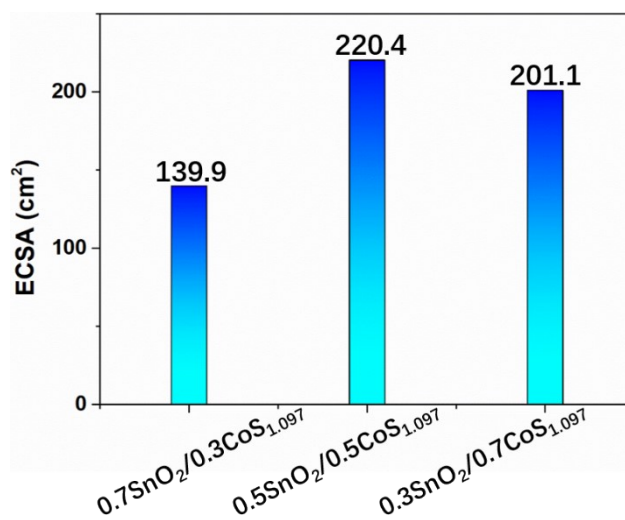


**Figure S11** The ECSA of 0.7 SnO<sub>2</sub>/0.3 CoS<sub>1.097</sub>, 0.5 SnO<sub>2</sub>/0.5 CoS<sub>1.097</sub>, and 0.3 SnO<sub>2</sub>/0.7 CoS<sub>1.097</sub>.



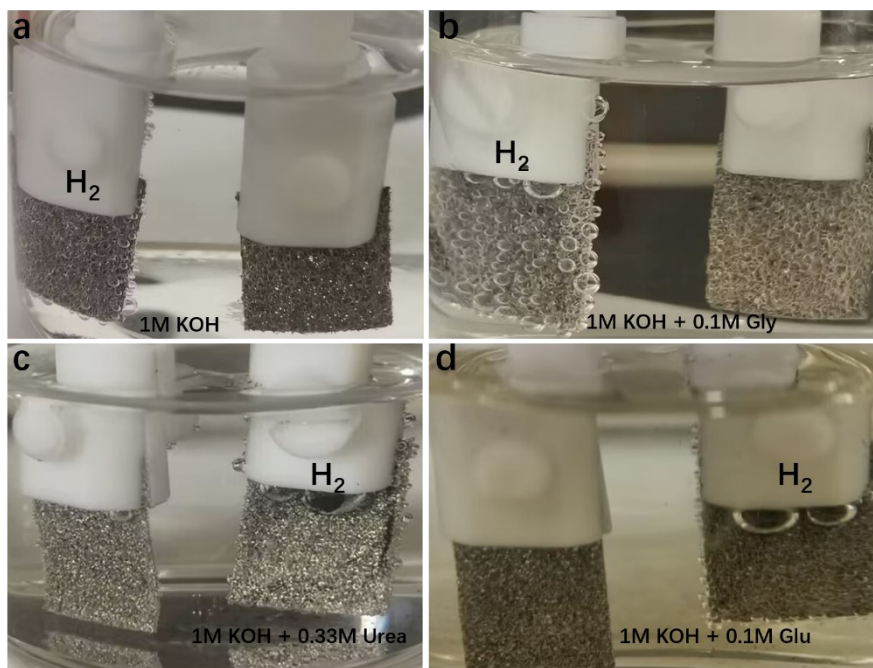


**Figure S12** The photos of overall water splitting of  $0.5 \text{ SnO}_2/0.5 \text{ CoS}_{1.097}$  in (a) 1 M KOH, (b) 1 M KOH + 0.1 M gly, (c) 1 M KOH + 0.33 M urea, and (d) 1 M KOH + 0.1 M glu.

## References

1. Z. Yang, X. Xie, Z. Zhang, J. Yang, C. Yu, S. Dong, M. Xiang and H. Qin, *Int. J. Hydrogen Energy*, 2022, 47, 27338-27346.
2. Z. Yang, X. Xie, J. Wei, Z. Zhang, C. Yu, S. Dong, B. Chen, Y. Wang, M. Xiang and H. Qin, *J. Colloid. Interface Sci.*, 2023, 642, 439-446.
3. X. Yu, R. B. Araujo, Z. Qiu, E. Campos dos Santos, A. Anil, A. Cornell, L. G. M. Pettersson and M. Johnsson, *Adv. Energy Mater.*, 2022, 12, 2103750.
4. G. Kresse and J. Furthmuller, *Comput. Mater. Sci.*, 1996, 6, 15-50.
5. P. E. Blöchl, *Phys. Rev. B* 1994, 50, 17953-17979.
6. J. P. Perdew, J. A. Chevary, S. H. Vosko, K. A. Jackson, M. R. Pederson, D. J. Singh and C. Fiolhais, *Phys. Rev. B* 1992, 46, 6671-6687.
7. L. Fan, Y. Ji, G. Wang, Z. Zhang, L. Yi, K. Chen, X. Liu and Z. Wen, *J. Energy Chem.*, 2022, 72, 424-431.
8. X. Liu, Z. Fang, X. Teng, Y. Niu, S. Gong, W. Chen, T. J. Meyer and Z. Chen, *J. Energy Chem.*, 2022, 72, 432-441.
9. H. Yu, W. Wang, Q. Mao, K. Deng, Z. Wang, Y. Xu, X. Li, H. Wang and L. Wang, *Appl. Catal., B*, 2023, 330, 122617.
10. S. Li, W. Xie, Y. Song, Y. Li, Y. Song, J. Li and M. Shao, *Chem. Eng. J.*, 2022, 437, 135473.
11. S. Ligani Fereja, P. Li, Z. Zhang, J. Guo, Z. Fang, Z. Li, S. He and W. Chen, *Chem. Eng. J.*, 2022, 432, 134274.
12. Y. Zhang, Y. Qiu, Z. Ma, Y. Wang, Y. Zhang, Y. Ying, Y. Jiang, Y. Zhu and S. Liu, *J. Mater. Chem. A*, 2021, 9, 10893–10908.
13. X. Liu, P. Cai, G. Wang and Z. Wen, *Int. J. Hydrogen Energy*, 2020, 45, 32940-32948.